Journal of Applied Polymer Science

Photodynamic antifungal activities of nanostructured fabrics grafted with rose bengal and phloxine B against *Aspergillus fumigatus*

Joo Ran Kim, Stephen Michielsen
Fiber and Polymer Science, Textile Engineering, Chemistry and Science, North Carolina State University, Raleigh, North Carolina
Correspondence to: S. Michielsen (E-mail: smichie@ncsu.edu)

ABSTRACT: This study demonstrates that nanostructured fabrics grafted with rose bengal (RB) and phloxine B (PB) have photodynamic antifungal effects on *Aspergillus fumigatus*. RB and PB were attached to vinyl benzyl chloride, and, subsequently, this was polymerized with acrylic acid and styrene sulfonic acid to produce long, water-soluble polymers to attach to the fabric surface. This gave high grafting yield and photodynamic antifungal activity against *A. fumigatus*. In RB and PB microdilution tests, there was no visible turbidity at 63 μmol/L. When polymerized RB and PB were incorporated into fabrics, the actions of polymerized RB and PB resulted in less hyphal growth and germination of conidia on *A. fumigatus* than the free RB and PB dyes. Nanostructured fabrics created by bonding RB- or PB-containing polymers to electrospun nylon mats exhibited higher concentrations of the dyes, equivalent to 86 μmol/L. The microstructured fabrics created by bonding RB- or PB-containing polymers to spunbonded nylon nonwoven fabrics only exhibited the equivalent of 32 μmol/L of the dyes. The nanostructured fabrics had a specific surface area of 28.1 m^2/g, whereas the microfabric had 1.5 m^2/g. Thus, the nanostructured fabrics increased the surface area 18.7× and the reflectance percent 16.2× when compared with the microstructured fabrics. This resulted in much higher photodynamic antifungal activity against *A. fumigatus*. © 2015 Wiley Periodicals, Inc. J. Appl. Polym. Sci. **2015**, *132*, 42114.

KEYWORDS: biomedical applications; biomaterials; nanostructured polymers; photochemistry; textiles

Received 3 November 2014; accepted 13 February 2015
DOI: 10.1002/app.42114

INTRODUCTION

Aspergillus fumigatus is an opportunistic fungus and is one of the most common species found in soil and dead organic materials.[1] It induces invasive aspergillosis in immunosuppressed patients, particularly patients with leukemia where 10–25% of all patients develop aspergillosis, resulting in a mortality rate of 80–90%.[1] In 2007, 1.3 million people were diagnosed with HIV/AIDS in the United States and 33.2 million people in the world.[2] Another 1.4 million patients have been diagnosed with malignancy in the United States.[3] The number of immunosuppressed patients increases annually, and they are highly susceptible to opportunistic fungi resulting in the risk of aspergillosis and pneumocytosis. *A. fumigatus* may also cause asthma and allergic sinusitis in healthy individuals.[4,5]

Recently, photodynamic therapy (PDT) has been investigated as a treatment for several biological pathogens. PDT uses a photosensitizer, which can be activated by exposure to visible light in a specific wavelength range to produce reactive oxygen species.[6] After a photosensitizer absorbs a photon in this wavelength range, an electronic transition occurs and the molecule is promoted to an excited singlet electronic state, usually the first excited singlet state, S_1.[7] Then, the excited molecule may return to the ground electronic state via fluorescence or internal conversion. Alternatively, it may undergo intersystem crossing to the triplet excited state (T_1 or T_2), which has a longer lifetime. The energy from the triplet state of the excited photosensitizer may then transfer its energy to a nearby ground-state oxygen molecule. This results in the conversion of the $^3O_2$ molecule to the singlet state of oxygen, $^1O_2$.[8] The $^1O_2$ reacts with biological cell membranes, in particular lipids such as fatty acids and ergosterol, to induce photooxidation. This in turn leads to cell damage and an increase in membrane permeability[8,9] via changes to the plasma membrane components, drastically inducing membrane dysfunction and K^+ leakage and resulting in fungal death.[10]

One class of dyes used in PDT is the xanthene dyes such as rose bengal (RB), phloxine B (PB), and erythrosin B. They are commonly used in the drug, food, cosmetic, and textile industries.[11] Xanthene dyes are approved as food additives in the United States, the European Union, and Japan, as shown in Figure 1 along with their structures and their quantum yields for producing singlet oxygen.[12] Xanthene dyes have been reported to induce photoinactivation due to the dye-sensitized formation of

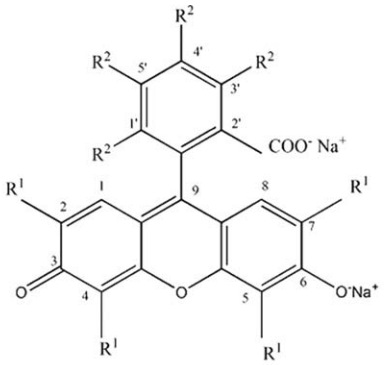

Xanthene dyes	R^1	R^2	Food additives	Quantum yield in H_2O
Rose Bengal	I	Cl	Food Red No. 105 in Japan	0.76
Phloxine B	Br	Cl	Food Red No.3 in Japan FD&C Red No.3 in USA E-127 in European Union	0.58

Figure 1. Chemical structures of xanthene dyes.[1]

reactive singlet oxygen, which oxidizes many biological molecules.[13,14] Numerous studies have shown antimicrobial activity in the *in vitro* destruction of bacteria, yeast, or fungi with xanthene dyes,[14–17] in particular, photodynamic treatment of the fungus *Candida albicans*.[18] However, there is little antifungal PDT research against opportunistic fungi such as *A. fumigatus* with xanthene dyes. In the work described below, the antifungal effects of fabrics grafted with RB or PB against *A. fumigatus* after photoirradiation are investigated.

EXPERIMENTAL

Materials

Aspergillus fumigatus (ATCC 13073) was donated by the United States Department of Agriculture, Agricultural Research Service, Peoria, IL, USA. PB, potato dextrose agar (PDA), RPMI 1640 medium, sterile water, 4-(4,6-dimethoxy-1,3,5-triazin-2-yl)−4-methylmorpholinium chloride (DMTMM), 3-(*N*-morpholino)-propanesulfonic acid (MOPS), Tween® 20, and nylon 6,6 pellets and formic acid (reagent grade > 95%) were purchased from Sigma Aldrich Chemical (St. Louis, MO, USA). The 0.5 McFarland standard was purchased from Fisher Scientific (Pittsburgh, PA, USA). The spunbonded nylon nonwoven fabric Cerex Spectramax® nylon 6,6 and RB dye were donated by LaamScience (Cary, NC, USA). The nonwoven fabric is referred to as "microfabric" below to contrast the size of the fibers from those in an electrospun nanofiber fabric, referred to as "nanofabric" below.

Polymerization of Xanthene Dye

The procedure described by Zhang[19] was followed to incorporate the xanthene dyes into a water-soluble polymer that could be grafted onto nylon fabric. The first step was the synthesis of vinyl benzyl-xanthene dyes (VBXT) monomer shown in Figure 2(a). RB or PB was reacted with 4-vinyl benzyl chloride in a three-necked round-bottomed flask in a solvent consisting of 34 mL of distill water and 35 mL of acetone. A reflux condenser was attached to prevent evaporation of acetone. The solution was heated on a water bath with stirring at 65°C for 3 h. The precipitated VBXT was filtered and washed several times with distilled water to remove acetone. The water was removed using vacuum drying. The second step was copolymerization of VBXT with acrylic acid (AA), which provides carboxylic groups to graft to nylon fabrics and 4-styrene sulfonic acid, which confers increased water solubility. The molar feed ratios of the monomers for the polymerization were 1 VBXT : 40 SSA : 140 AA, and the final polymer is depicted in Figure 2(b). Specifically, the VBXT monomer and AA were dissolved in the solvent of acetone and distilled water solution at a molar ratio of 1 : 140. Then, 0.03 g of sodium metabisulfite and 0.03 g of ammonium persulfate were added as initiators, and the reaction mixture was stirred for 1 h. Finally, this solution was transferred to another beaker which contained SSA aqueous solution, and the polymerization was continued with stirring at 65°C for an additional 1 h. Poly(acrylic acid-*co*-styrene sulfonic acid-*co*-vinyl benzyl chloride rose bengal), PBRB, and poly(acrylic acid-*co*-styrene sulfonic acid-*co*-vinyl benzyl chloride phloxine B), PBPB, were produced.[19] The amine end groups of nylon can react with carboxylic acid group of polymerized dye solutions to produce covalent amide linkages resulting in a high grafting yield.[20]

Electrospinning

Nanostructured nylon fabric was prepared via electrospinning. First, nylon 6,6 pellets were dissolved at 18 wt % in formic acid

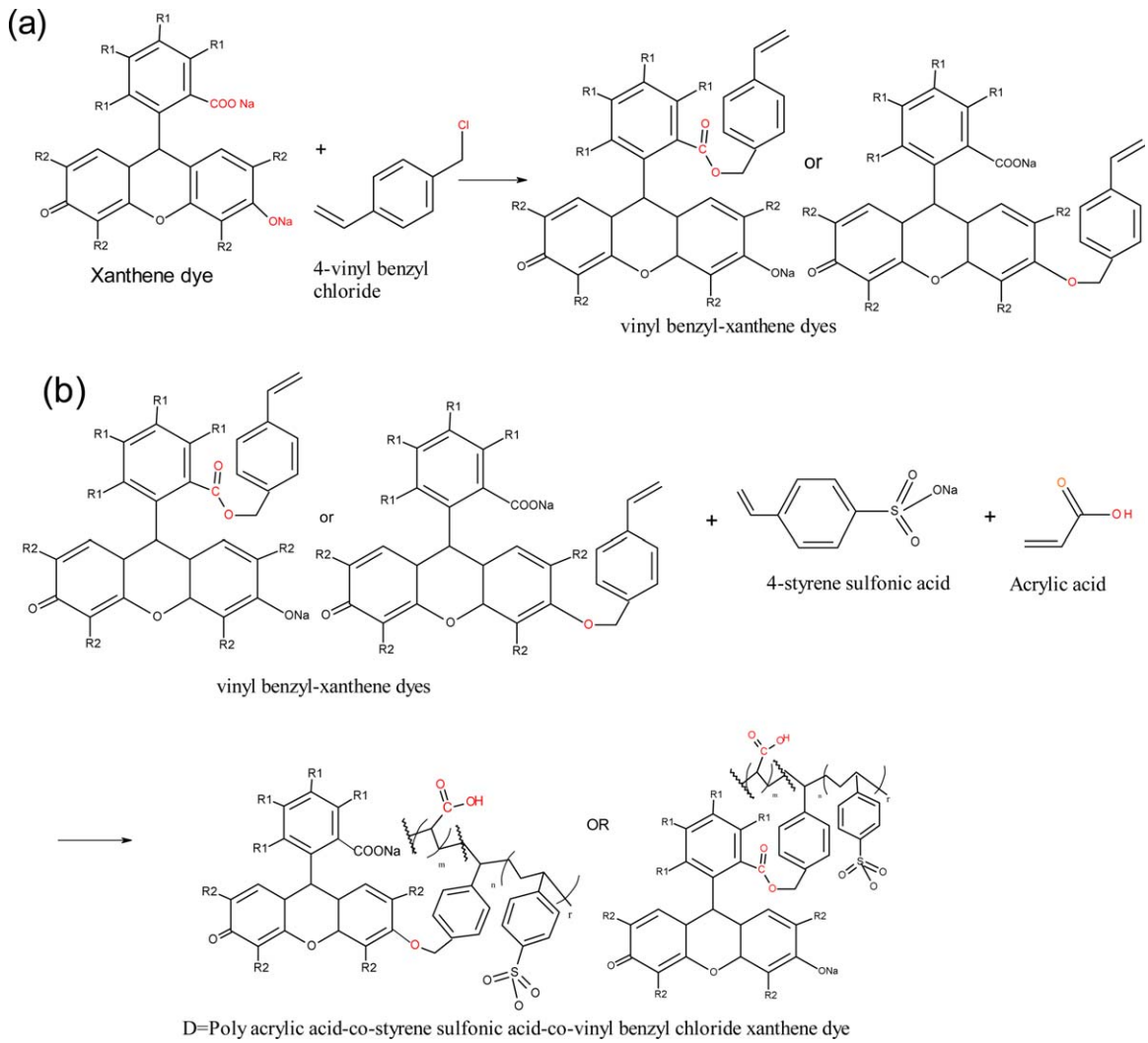

Figure 2. Polymerization procedures of poly(acrylic acid-*co*-styrene sulfonic acid-*co*-vinyl benzyl chloride xanthene dye): (a) synthesis of vinyl benzyl xanthene dyes, and (b) copolymerization of PBRB or PBPB having two possible structures.[2] The amine group of nylon 6,6 can react with carboxylic acid group of polymerized dye solutions producing amide linkage, R_1 is Cl and R_2 is I for rose bengal, whereas R_1 is Cl and R_2 is Br for phloxine B. [Color figure can be viewed in the online issue, which is available at wileyonlinelibrary.com.]

at 70°C with stirring for 8 h. The solution was placed into a 10-mL syringe and then placed on a syringe pump. The feeding rate of solution was 1 mL/h. A high voltage of 20 kV was applied between the needle tip and the roller collector as shown in Figure 3.

Grafting Photochemicals to Fabrics

The aluminum foil coated with electrospun nylon fibers was carefully wrapped onto glass microscope slides. These slides and spunbonded nylon nonwoven fabrics were placed into 100 μmol/L aqueous solutions of RB, PB, and aqueous solutions of PBRB and PBPB. Then, 0.3 g of DMTMM coupling agent was added to the solution. The fabric was taken from the solution after 12 h and placed into an oven (Werner Mathis AG LTF 134489, Concord, NC, USA) for 5 min at 170°C.

Preparation of Inoculum

A. fumigatus was inoculated on PDA dish and was cultured at 35°C for 7 days. RPMI-1640 sterile media with 0.2% glucose was buffered to a pH of 7.0 with 0.165 mol/L MOPS, and 0.01% wetting agent Tween® 20 was added. This solution was added to fungi cultures. Then, the cultures were scraped to separate the spores from the remainder of the fungi biomass and filtered using Millipore® polytetrafluoroethylene film with 5 μm pore size.

Broth Microdilution Tests

A modified CLSI M38-A standard designates a broth microdilution method for testing antifungal susceptibility of filamentous

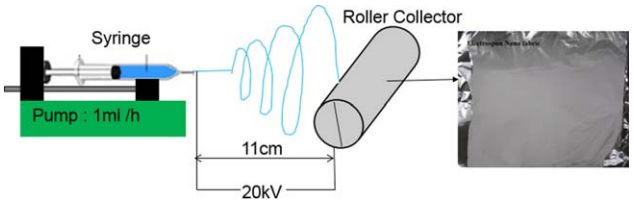

Figure 3. Schematic of electrospinning of nylon 6,6. [Color figure can be viewed in the online issue, which is available at wileyonlinelibrary.com.]

fungi.[21] In the broth microdilution method, the inoculum preparation of conidia of *A. fumigatus* was adjusted using 0.5 McFarland standard by counting the number of spores counted using a hemocytometer and adding the broth until the concentration was in the range of 2×10^6 CFU/mL. RB, PB, PBRB, and PBPB were diluted by a series of twofold dilutions to obtain solutions from 1 to 500 μmol. Next, 100 μL of these solutions were placed into each well of the microdilution tray. Then, 100 μL of the prepared inoculum was deposited into each well. The tray was placed under a 200-watt incandescent lamp. A pyrex glass dish filled with water was placed between the lamp and the microdilution tray to absorb infrared light from a photoflood lamp (Smith Victor, Griffith, IN, USA) to avoid heating the tray. The light intensity was measured using a digital illuminance meter (Model LX1330B, Union City, CA, USA) at 16,000 Lux. After 5-h photoirradiation, the tray was incubated at 35°C for 48 h, and the turbidity and growth of fungi in each well were observed and compared with a growth control and a sterile control in the last two rows of the microdilution tray. In this test, the minimum inhibitory concentration (MIC) could be obtained by observing which wells exhibited no noticeable growth (optically clear or no turbidity) as observed visually.

Inhibition Zone Tests of Fabrics Grafted with Photosensitizers, RB, and PB

The 100-μL inoculum of *A. fumigatus* prepared above at 2×10^6 CFU/mL was transferred to PDA plates, and then each of the 5×5 cm^2 of antifungal fabrics previously grafted with RB, PB, PBRB, and PBPB was placed on the PDA. The PDA plates were kept under the same lamp used above for 5 h (with irradiation) or in the dark (without irradiation). The PDA plates were taken and then incubated for 7 days in the dark at 35°C. After incubation, the inhibition zone of the fabrics was observed.

Absorption Spectra of Dyes

Aqueous solutions of RB and PB at a concentration from 8 to 1000 µmol/L and polymerized PBRB and PBPB were prepared in deionized water. Next, 2 mL of the dye solutions were transferred into 24-well Biofil® tissue culture plates, which were then placed in a Biotek® Synergy HT multimode reader to measure the maximum optical absorption.

Investigation of Structures

A Thermo Electron FTIR with Nexus 470 bench and Continuum Microscope (Nicolet Instrument Technologies, Fitchburg, WI, USA) was used to investigate the structures of VBRB and VBPB. The specific surface areas of nanostructured nylon 6,6 and microstructured fabrics were measured by applying the Brunauer–Emmett–Teller (BET) analysis using a Gemini VII 2390p physisorption analyzer from Micrometrics coupled with SmartPrep 065 degassing unit (Micromeritics Instrument, Norcross, GA, USA). The glass tube was weighed, and then 0.5 g of fabric sample was placed into the glass tube and degassed at 150°C under nitrogen gas flow and covered with a rubber lid for 2 h. Then, the glass tube was weighed to obtain the sample weight after degassing. An empty glass tube was used as the control, and the sample tubes were placed above liquid nitrogen in an analyzer. Next, the tubes were evacuated using helium gas as a flush gas and refilled with nitrogen gas. In physical adsorption, there is a weak Van der Waals attraction between the adsorbate (nitrogen) and the solid surface. To investigate the specific surface area, the amount of nitrogen adsorbed on the fabrics was calculated using the following equation:

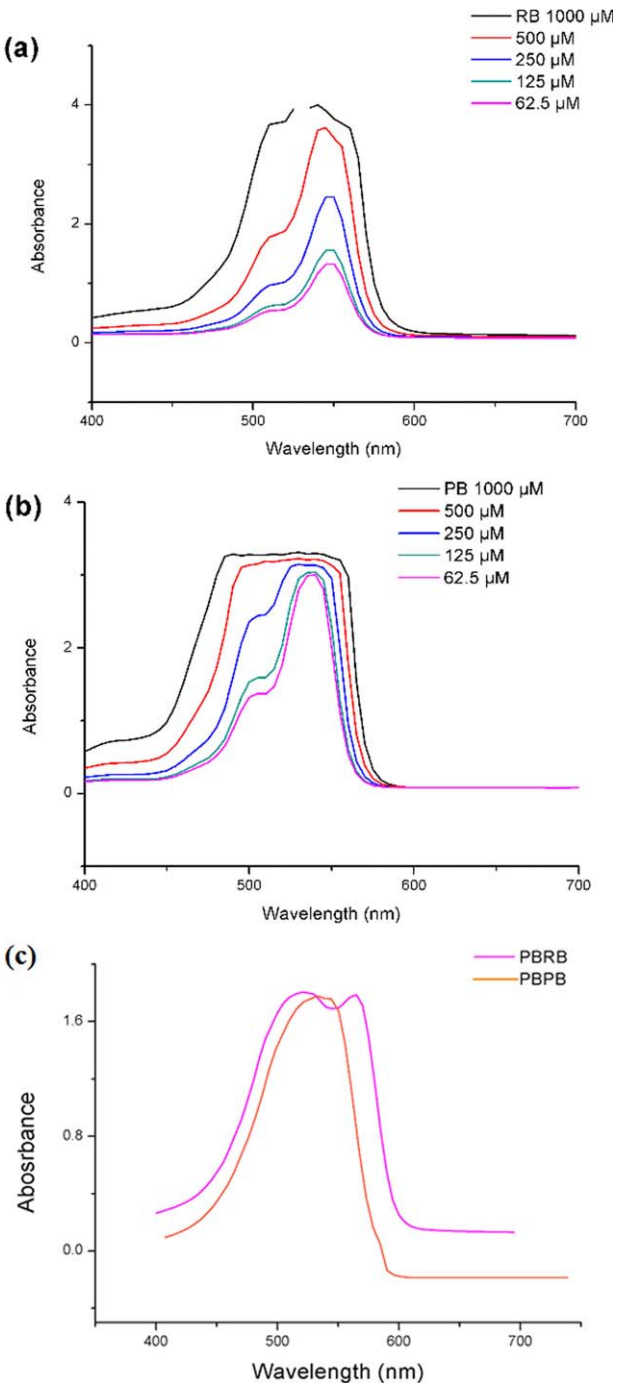

Figure 4. Absorbance spectra of photochemical dyes for wavelengths 400–700 nm at different concentrations: (a) rose bengal, (b) phloxine B, and (c) PBRB and PBPB. [Color figure can be viewed in the online issue, which is available at wileyonlinelibrary.com.]

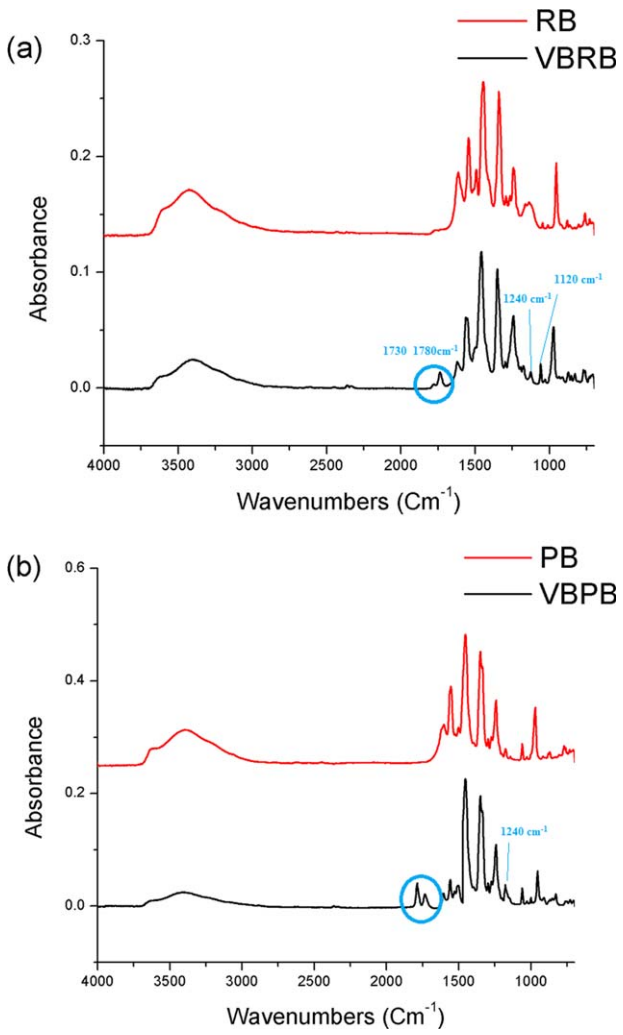

Figure 5. FTIR absorbance spectra of (a) RB and VBRB and (b) PB and VBPB. [Color figure can be viewed in the online issue, which is available at wileyonlinelibrary.com.]

$$\frac{1}{W((P_0-P)-1)}=\frac{1}{W_mC}+\frac{C-1}{W_mC}\left(\frac{P}{P_0}\right), \quad (1)$$

where W is the weight of gas absorbed, P/P_0 is the relative pressure, W_m is the weight of adsorbate in a monolayer, and C is the BET constant.[22]

Colorimetric Test

The nanoscale and microscale fabrics grafted with PBRB and PBPB were prepared by stacking at least 16 layers for microstructured fabrics and five layers for nanostructured fabrics. Then, the reflectance was measured from 360 to 700 nm twice and repeated in four different spots on each sample using a Datacolor SF600X (Lawrenceville, NJ, USA) spectrophotometer.

RESULTS AND DISCUSSION

Absorbance of RB, PB, PBRB, and PBPB

The visible light absorbance of the photosensitized dyes was measured over the wavelength range 400–700 nm. Figure 3 shows the spectra of RB (maximum absorption at 550 nm) and PB ($\lambda_{max} = 540$ nm).

After polymerization of VBXT, PBRB had a broad spectrum with two absorbance maxima at $\lambda_{max} = 525$ and 565 nm, whereas PBPB showed only a slight shift from PB, that is, from 540 to 530 nm. It has been reported that the methylation or aggregation of xanthene dyes results in a broad absorption spectrum, and the shifts in the maximum wavelength are shown in Figure 4.

The C-6 and C-2′ position carbons in the xanthene dyes (see Figure 1) enable the coupling of the dyes to the methyl group of the vinyl benzyl moiety, which permits subsequent incorporation into the AA–SSA copolymer. The resulting terpolymer allows the dye molecules to be grafted to the fabrics through this coupling polymer. In previous studies of the esterification and etherification of xanthene dyes at C-6 and C-2′, respectively, the coupled dyes exhibit a shift in the absorption maximum wavelengths from 558 to 568 nm (C-6) and 518 to 528 nm (C-2′).[23,24] PBRB showed a broader absorbance region than RB and a shift in the spectrum, leading to a pair of peaks of equal intensity at 525 and 565 nm. We also found that the absorption spectra of RB and PB depended on dye concentration, which has been attributed to the aggregation of dye molecules at high concentrations. The aggregation of dyes also results in a shift of the maximum wavelengths.

Figure 5 shows the FTIR results for RB, PB, VBRB, and VBPB. The FTIR spectrum of VBRB has new peaks at 1730 and 1780 cm^{-1} that do not occur in RB [Figure 5(a)], which indicates C═O ester bonds in its structure. In addition, there is an increase in absorbance at 1120 cm^{-1}, which is due to aliphatic ether C—O bonds. Similar results are observed for PBPB, as shown in Figure 5(b), where VBPB also showed peaks at 1730 and 1780 cm^{-1} and showed a peak at 1240 cm^{-1}, which indicates the presence of aromatic ether C—O bonds. RB and PB may attach to the methyl group of the vinyl benzyl moiety at both the C-2′ and C-6 locations. PB showed less change at 1120 cm^{-1} than RB; however, it exhibits a strong peak at 1240 cm^{-1}. PB may be more likely to get attached at C-2′

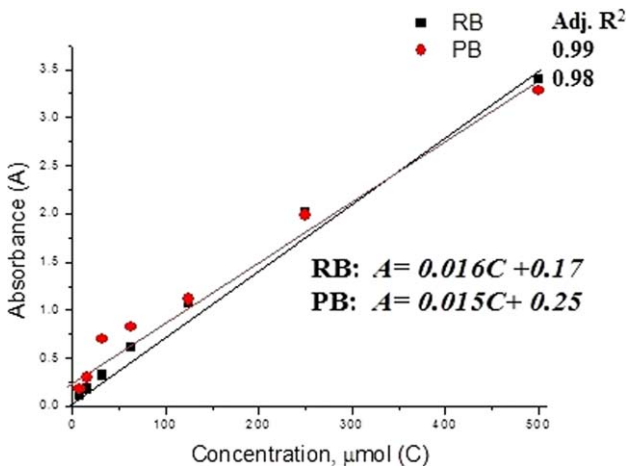

Figure 6. Linear regression relationships between concentration and absorbance from 8 to 500 µmol/L in free dye solutions of RB and PB, where C is given in μmol/L. [Color figure can be viewed in the online issue, which is available at wileyonlinelibrary.com.]

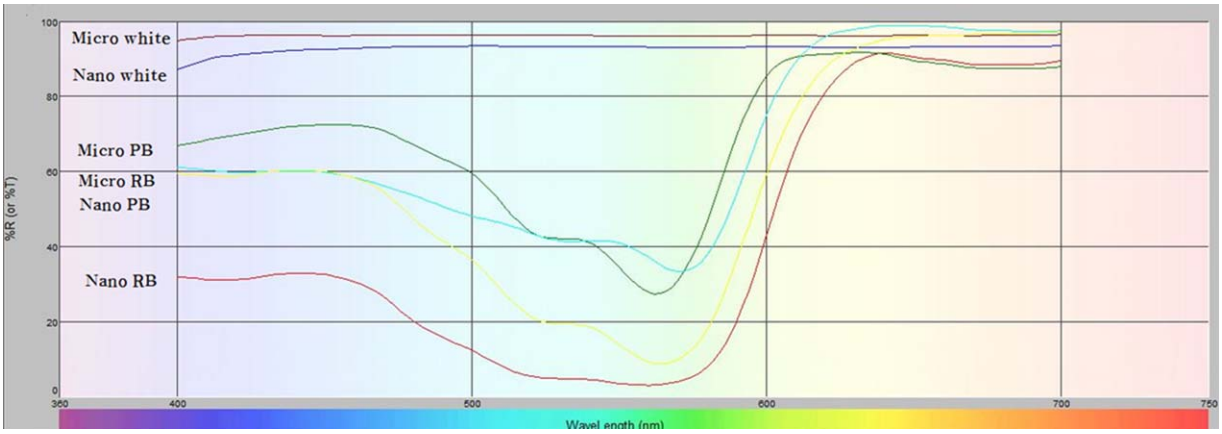

Figure 7. The reflectance percent of microstructured and nanostructured fabrics grafted with polymerized RB and PB, micro and nano white are control fabrics without dye. Microstructured fabrics grafted with RB and PB show higher reflectance percent than nanostructured fabrics grafted with RB and PB. %*R* is percent reflectance. [Color figure can be viewed in the online issue, which is available at wileyonlinelibrary.com.]

position and form the lactone, which is the closed ring form because the quinoid form (open ring) of PB may be less stable in acidic conditions encountered during polymerization.[25,26]

Analysis of the Amount of Grafted Photosensitizers

We measured the absorbance of each photosensitizer as a function of the concentration from 8 to 1000 μM for RB and PB (Figure 4) and fit the Beer-Lambert Law ($A = \varepsilon cl$, where A is absorbance, ε is the absorptivity, c is concentration, and l is the path length) to it (Figure 6). To estimate the concentration of dye on the fabrics, we assumed that the absorptivity was unchanged by incorporating the dye into the polymer, PBRB or PBPB. We then measured the reflectance from the fabrics (Figure 7) and used the following equation to obtain the amount of dye on the fabrics:

$$A = 2 - \log_{10} R, \tag{2}$$

where A is absorbance and R is percent reflectance. From the absorbance, we then obtained the equivalent concentration as given in Table I. The nanostructured fabrics grafted with PBRB and PBPB exhibited higher equivalent grafting concentration resulting in 86 and 82 μmol/L of RB or PB within the polymer, whereas the microstructured fabrics exhibited much lower effective grafting concentration bound with dye molecules resulting in 32 and 28 μmol/L of RB or PB.

However, this method is limited by light scattering off the fabrics and the absorption of the light. Therefore, we also measured the K/S values of the fabrics and used the Kubelka-Munk equation [eq. (3)] to get the color strength (Table I). K/S is proportional to the concentration of dye on the fabrics. The nanostructured fabrics show higher K/S values at lower reflectance percent.

$$\frac{K}{S} = \frac{(1 - R_\infty)^2}{2R_\infty} = F(R_\infty), \tag{3}$$

where K and S are absorption and scattering coefficients (cm^{-1}), respectively, R_∞ is the reflectance of infinite thickness, if the fabric is sufficiently of opaque thickness, and $R_{max} = R_\infty$ at maximum wavelength.[27]

The K/S values were converted to relative color strength (%) using the following equation:[28]

$$\textit{Relative} \text{ color strength } (\%) = \frac{K/S \text{ of treated fabric}}{K/S \text{ of untreated fabric}} \times 100. \tag{4}$$

Nanostructured fabric grafted with PBRB and PBPB exhibited 80.5% and 51% relative color strength, respectively, whereas the microstructured fabric grafted with PBRB and PBPB showed only 5% relative color strength when compared with untreated fabric sample. In other words, there was approximately 16× RB or 10× PB on the nanostructured fabrics when compared with the microstructured fabrics.

Specific Surface Area of Nanostructured Fabrics

Figure 8 shows SEM images of microfabrics and nanofabrics showing the different fiber sizes in the two fabrics. From the images, nanofibers had diameters in the range of 200–550 nm, whereas the microfibers had diameters in the range from 12 to 20 μm. By using BET analysis, the specific surface area of microfabrics and nanofabrics was calculated according to eq. (1). The nanofabrics had a specific surface area of 28.1 m^2/g,

Table I. Percent Reflectance, Absorbance at λ_{max}, and Concentrations of Nanostructured and Microstructured Fabrics Grafted with RB or PB

	Reflectance (%) at λ_{max}		Absorbance		Concentration (μmol/L)		$F(R_\infty)$		Color strength (%)	
Grafting agent	Nano	Micro	Nano	Micro	Nano	Micro	Nano	Micro	Nano	Micro
RB	2.93	21.22	1.53	0.67	85.79	31.68	0.16	0.015	80.50	5.00
PB	3.07	20.7	1.47	0.68	81.11	27.87	0.15	0.015	51.00	5.00

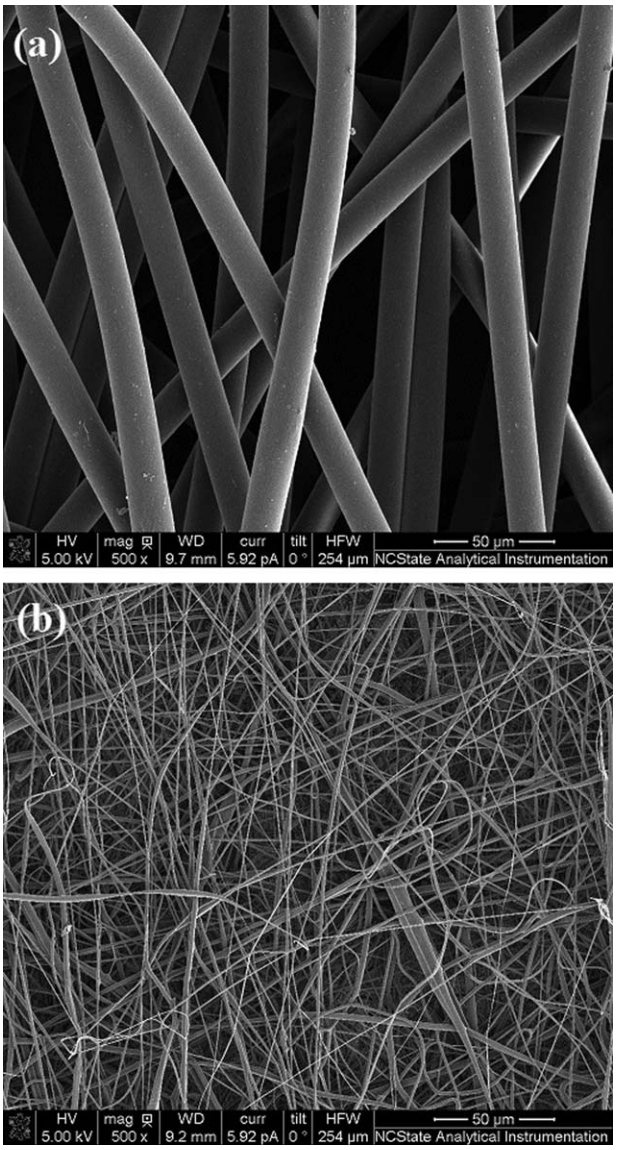

Figure 8. Scanning electronic microscopic images of microstructured and nanostructured nylon 6,6 fabrics: (a) microfibers and (b) nanofibers. The bar scale is 50 µm.

whereas the microfabric had 1.5 m^2/g. Thus, the nanofabrics had 18.7× the surface area as the microfabrics. This result agrees well with color strength measurements given above.

Photoactive Antifungal Test: Broth Microdilution

In the broth microdilution test, RB, PB, PBRB, and PBPB were diluted by a series of twofold dilutions starting with a concentration of 500 µmol/L (RB and PB) and the equivalent absorbance for PBRB and PBPB. After 48-h incubation at 35°C, all wells at concentrations below 32 µmol/L of RB and PB showed visible growth of hyphae and turbidity (Figure 9). For RB and PB, there was no visible turbidity or growth at a concentration of 63 µmol/L or higher, whereas concentrations below 63 µmol/L showed visible hyphal growth. PBRB exhibited a MIC equivalent to 125 µmol/L of RB, whereas PBPB exhibited a MIC equivalent to 250 µmol/L of PB. The wells circled in Figure 9 indicate the MIC, which is the lowest concentration that inhibits more than 95% of the fungi growth. The MIC of RB, PBRB, PB, and PBPB for three replicates is summarized in Table II. RB and PB exhibited MIC at 53 and 63 µmol/L, whereas PBRB and PBPB showed equivalent MICs of 104 and 250 µmol/L, respectively.

Based on these broth microdilution tests, PBRB was more effective than PBPB. This is consistent with the quantum yields for producing singlet oxygen by RB (quantum yield = 0.76) and PB (quantum yield = 0.58).[29] This is because RB has the heaviest halogens in its structure, which increases the yield of intersystem crossing to the triplet state to give more of the reactive singlet oxygen.[8]

Photodynamic Antifungal Fabric Test

Finally, we preformed the zone of inhibition test on fabrics treated with RB, PB, PBRB, and PBPB. The zone of inhibition is a clear zone with no growth surrounding the test fabric. To observe a zone of inhibition, the active agent must diffuse away from the treated fabric such that, within the zone, the concentration of the antifungal agent exceeds the MIC. If the antifungal agent is bound to the fabric, there should not be any zone of inhibition. However, the fungi in direct contact with the treated fabric may still experience the photodynamic antifungal effects. Figure 10 shows the zone of inhibition test for an untreated fabric, fabric treated with solutions of RB and PB,

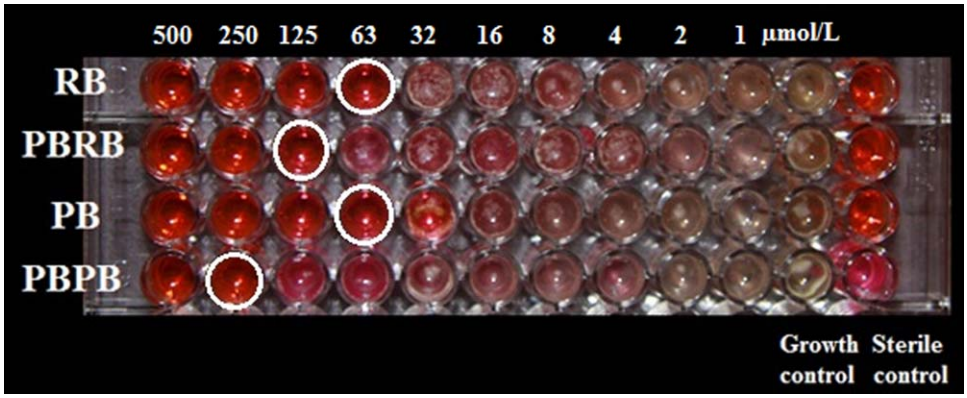

Figure 9. Broth microdilution test of RB, PB, PBRB, and PBPB solutions against *A. fumigatus*: free dyes RB and PB have MIC of 63 µmol/L, and PBRB and PBPB exhibited MIC at equivalent concentrations of 125 and 250 µmol/L, respectively. [Color figure can be viewed in the online issue, which is available at wileyonlinelibrary.com.]

Table II. Minimum Inhibitory Concentration (MIC) for RB and PB or Equivalent Concentrations Based on the Absorbance for PBRB and PBPB (in μmol/L)

Test	RB	PBRB	PB	PBPB
First	63	125	63	250
Second	32	63	63	250
Third	63	125	63	250
Final MIC	53	104	63	250

and fabrics treated with PBRB and PBPB, where the polymers were covalently bonded to the fabric in the 5-h irradiation or nonirradiation conditions. The inhibition zone test examined visible growth of hyphae and germination around the fabrics. Figure 10(b–g) shows the results after 5-h irradiation, and Figure 10(h–m) exhibits the inhibition zone in the nonirradiation condition. All samples under the nonirradiation exhibited fungal growth that covered the entire fabric surface. The activity of treated antifungal fabrics showed little or no zone of inhibition around the fabrics. As the antifungal agent photodynamically produced singlet oxygen, and as singlet oxygen has a short lifetime, it has limited diffusivity, allowing singlet oxygen to diffuse only ~ 0.1 mm.[30] Thus, no zone of inhibition would be expected if the dyes were chemically bonded to the fabrics.

Figure 10(f,g) shows that there is no zone of inhibition for the nanostructured fabrics treated with PBRB and PBPB; however, there is no *A. fumigatus* growth on the fabrics. This indicates that PBRB and PBPB are bonded to the surface and sufficient singlet oxygen is produced under visible light illumination to prevent *A. fumigatus* growth. Similar results are shown in Figure 10(d,e) for the microstructured PBRB- and PBPB-treated fabrics; however, there is some germination and hyphal growth and a few fungal colonies on the fabric surface. As the amount of PBRB and PBPB on these fabrics is ~ 1/16th of the amount on the nanostructured fabrics, less fungal inhibition would be expected. In Figure 10(b,c), the fabrics treated with RB and PB dyes showed *A. fumigatus* growth above and below fabrics. These dyes were not bonded to the surface and the color nearly disappeared after 5-h illumination. This is because nonpermanent chemical bonds allowed the dyes to diffuse away, resulting in a lower concentration on fabric surfaces. We suggest that the lack of a zone of inhibition for these two fabrics is simply because of their low concentration in the zone around the fabrics. The diffusion away from the fabrics would result in a loss of color from the fabrics, as observed. Finally, the untreated control fabric was completely covered with hyphal growth and germination on the fabric, exhibiting no antifungal behavior, just as one would expect. In additional studies, similar antifungal activity against *Phytophthora cinnamomi*, *Trichoderma viride*, *Aspergillus niger*,

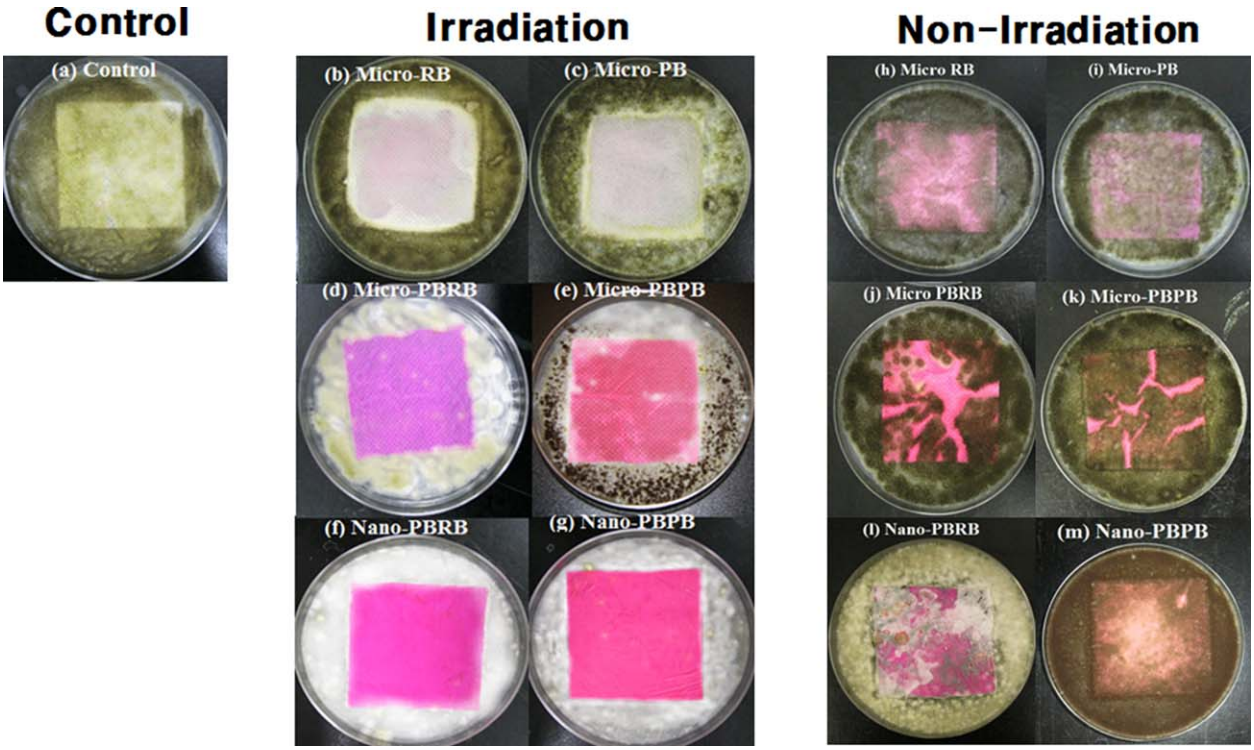

Figure 10. Antifungal fabric tests of (a) control, (b) microstructured fabric with RB, (c) microstructured fabric with PB, (d) microstructured fabric with PBRB, (e) microstructured fabric with PBPB, (f) nanostructured fabric with PBRB, and (g) nanostructured fabric with PBPB in the irradiated condition when compared with the same fabrics in the dark (h–m). Microstructured fabric with RB and PB applied but not covalently attached (b and c) exhibit fungal growth above and below the fabric and more color fading than the fabric grafted with PBRB and PBPB (d and e). Nanostructured fabrics in the bottom row show less germination and hyphal growth on the fabric surface when compared with microstructured fabrics. The results (h–m) tested in the dark shows that the fungal growth covered the entire fabric surface in all microstructured and nanostructured fabrics grafted with RB, PB, PBRB, and PBPB. [Color figure can be viewed in the online issue, which is available at wileyonlinelibrary.com.]

Chaetosphaeridium globosum, *Penicillium funiculosum*, and *Magnaporthe grisea* was observed on these antifungal fabrics.[31] In general, the nanofabrics grafted with PBRB and PBPB showed higher inactivation of *A. fumigatus* when compared with the microstructured fabrics.

CONCLUSIONS

The incorporation of RB and PB into a polymer via free radical copolymerization enables RB and PB to be grafted onto fabric surfaces to give high grafting yield and enhanced photodynamic antifungal activity against *A. fumigatus*. From broth microdilution, we found that PBRB produced more inactivation than PBPB on *A. fumigtus*. In the inhibition zone test, the fabrics grafted with PBRB also have higher inhibition than the fabrics grafted with PBPB. This is because RB has higher quantum yield for producing singlet oxygen, the antifungal agent. By comparing the photodynamic antifungal activity of microstructured and nanostructured fabrics, the nanostructured fabrics bound with RB or PB had higher concentrations resulting in equivalent concentrations of 86 and 82 μmol/L of RB or PB than the microstructured fabrics due to higher specific surface area (28.1 m^2/g). The higher specific surface area gave more sites to attach polymers onto the surface of fabrics. The nanostructured fabrics had 18.7× the surface area of the microstructured fabrics and 16.2× the reflectance percent of the microstructured fabrics.

In this study, the antifungal agent is singlet oxygen produced photodynamically by irradiation of RB or PB. As the dye is a permanent part of the polymer that has been covalently attached to the fabric, the zone of inhibition around the fabric is limited to the diffusion distance of singlet oxygen, which is $\sim 100\ \mu m$ in air and less in the presence of liquids. In other words, the photodynamic antifungal activity is limited to the surface of the fabric. These new photodynamic fabrics can be used in various applications, such as food packaging, air filters, upholstery, which is easily susceptible to biohazards, and medical textiles, for example, masks and surgical gowns. Further detailed study of the fabric grafted with xanthene dyes is required for long-term use.

ACKNOWLEDGMENTS

The authors thank Dr. W. Zhang for assistance in making the polymers and Ms. Meltem for assistance in electrospinning at NCSU College of Textiles. The authors also thank Dr. Margaret Daub at NCSU Plant and Microbial Biology for helpful discussion. This study was funded by LaamScience (Cary, NC, USA) and the College of Textile at North Carolina State University.

REFERENCES

1. Abbott, D. *Analyst* **1962**, *87*, 286.
2. World Health Organization. Global tuberculosis control: WHO Report. Global Tuberculosis Programme; World Health Organization: Geneva, **2010**.
3. Wolfe, R.; Roys, E.; Merion, R. *Am. J. Transplant.* **2010**, *10*, 961.
4. Abdel-Hafez, S.; Moubasher, A.; Shoreit, A.; Ismail, M. *J. Basic Microbiol.* **2007**, *30*, 467.
5. Chaudhary, N.; Marr, K. A. *Clin. Transl. Allergy* **2011**, *1*, 4.
6. Lyon, J. P.; Moreira, L. M.; de Moraes, P. C. G.; dos Santos, F. V.; de Resende, M. A. *Mycoses* **2011**, *54*, e265.
7. Dougherty, T. J.; Gomer, C. J.; Henderson, B. W.; Jori, G.; Kessel, D.; Korbelik, M.; Moan, J.; Peng, Q. *J. Natl. Cancer Inst.* **1998**, *90*, 889.
8. Ogilby, P. R. *Chem. Soc. Rev.* **2010**, *39*, 3181.
9. Phillips, D. *Pure Appl. Chem.* **1995**, *67*, 117.
10. DeRosa, M. C.; Crutchley, R. J. *Coord. Chem. Rev.* **2002**, *233*, 351.
11. Arthur, L. In Light-Activated Pest Control; Heitz, J., Downum, K., Eds.; American Chemical Society: Washington, D.C., **2005**; Chapter 4, pp 34–53.
12. Murov, S. L.; Hug, G. L.; Carmichael, I. Handbook of Photochemistry; Prodi, L., Gandolfi, T., Eds.; CRC Press: Boca Raton, **1993**; pp 41–43.
13. Kato, H.; Komagoe, K.; Nakanishi, Y.; Inoue, T.; Katsu, T. *Photochem. Photobiol.* **2012**, *88*, 423.
14. Waite, J. G.; Yousef, A. E. *Adv. Appl. Microbiol.* **2009**, *69*, 79.
15. Donnelly, R. F.; McCarron, P. A.; Tunney, M. M. *Microbiol. Res.* **2008**, *163*, 1.
16. Lyon, J. P.; de Maria Pedroso e Silva Azevedo, C.; Moreira, L. M.; de Lima, C. J.; de Resende, M. A. *Mycopathologia* **2011**, *172*, 293.
17. Walsh, T.; Viviani, M. A.; Arathoon, E.; Chiou, C.; Ghannoum, M.; Groll, A.; Odds, F. *Med. Mycol.* **2000**, *38*, 335.
18. Dai, T.; Fuchs, B. B.; Coleman, J. J.; Prates, R. A.; Astrakas, C.; St. Denis, T. G.; Ribeiro, M. S.; Mylonakis, E.; Hamblin, M. R.; Tegos, G. P. *Front. Microbiol.* **2012**, *3*, 120.
19. Zhang, W. The Study of the Synthesis of a Water Soluble Antimicrobial Polymer, Master Thesis, North Carolina State University, Raleigh, NC, May, **2012**.
20. Sherrill, J.; Michielsen, S.; Stojiljkovic, I. *J. Polym. Sci. Part A: Polym. Chem.* **2003**, *41*, 41.
21. Schwalbe, R.; Steele-Moore, L.; Goodwin, A. C. Eds. Antimicrobial Susceptibility Testing Protocols; CRC Press: Boca Raton, **2007**; Chapter 9, pp 173–208.
22. Brunauer, S.; Emmett, P. H.; Teller, E. *J. Am. Chem. Soc.* **1938**, *60*, 309.
23. Couch, B. C.; Kohn, L. M. *Mycologia* **2002**, *94*, 683.
24. Paczkowski, J.; Lamberts, J.; Paczkowska, B.; Neckers, D. *J. Free Radicals Biol. Med.* **1985**, *1*, 341.
25. Neckers, D. J. *Photochem. Photobiol. A: Chem.* **1989**, *47*, 1.
26. Valdes-Aguilera, O.; Neckers, D. *Acc. Chem. Res.* **1989**, *22*, 171.
27. Kubelka, P. Z. *Tech. Phys.* **1931**, *12*, 539.
28. Dev, V.; Venugopal, J.; Sudha, S.; Deepika, G.; Ramakrishna, S. *Carbohydr. Polym.* **2009**, *75*, 646.
29. Usui, Y. *Chem. Lett.* **1973**, *2*, 743.
30. Moan, J. *J. Photochem. Photobiol. B: Biol.* **1990**, *6*, 343.
31. Kim, J. R. The Photodynamic Antifungal Activity of Immobilized Xanthene and Thiazine Dyes on Electrospun Nano Nylon 6,6, Doctoral Thesis, North Carolina State University, Raleigh, NC, May, **2014**.